Bursts During November 1989 to January 1990

M. J. McPhaden,[1] F. Bahr,[2] Y. du Penhoat,[3] E. Firing,[4] S. P. Hayes,[1] P. P. Niiler,[5]
P. L. Richardson,[2] and J. M. Toole[2]

Several 5 to 10 m s^{-1} westerly wind bursts of 10–15 days' duration occurred in the western equatorial Pacific during November 1989 to January 1990. The response to these wind bursts was characterized by a 400- to 600-km-wide eastward jet in the upper 100–150 m along the equator between 135°E and the date line. Flow in this jet accelerated to speeds of over 100 cm s^{-1} within 1 week after the onset of westerly winds in November 1989 in association with supertyphoon Irma. In addition, a 20 to 40 cm s^{-1} westward counterflow developed between 2°N and 2°S below the surface jet separating it from the eastward flow of the Equatorial Undercurrent in the thermocline. Changes in surface layer zonal volume transports in the western Pacific due to westerly wind bursts were 25–56 Sv based on comparison of three shipboard velocity transects in November and December 1989. Although fluctuations in current speeds in the thermocline were generally smaller and less directly related to local wind forcing than those in the surface layer, the Equatorial Undercurrent decelerated to less than 20 cm s^{-1} (i.e., less than half its speed before the onset of westerlies) by early December 1989. Westerly winds also produced a strong surface convergence in both the meridional and zonal directions west of the date line. In late November 1989, this convergence was associated with downwelling of 2–3 m d^{-1} along the equator, and a 20- to 30-m depression of the thermocline. In addition, sea level rose by 10 dyn cm from mid-November to mid-December between 1°S and 3°N, 165°E. Sea surface temperature dropped over a large region by 0.2°–0.5°C during episodes of high westerly winds, and some episodes of high winds were associated with 0.2°–0.3°C sea surface temperature inversions supported by salt-stratified buoyancy gradients in the upper 100 m. The near-surface salinity balance was dominated by lateral advection when relatively fresh water from north of a salinity front centered near 3°N was advected southward by Ekman drift in late November 1989. Displacement of this front past a current meter mooring at 0°, 165°E, appeared as a local drop of 1 psu in surface layer salinity in 10 days. These results are discussed in the context of a swing in the climate system towards El Niño–Southern Oscillation-like conditions in early 1990.

1. Introduction

The general circulation of the atmosphere in the western equatorial Pacific is characterized by seasonally reversing monsoon winds west of 160°E, and weak trade winds between 160°E and the date line. Superimposed on the general circulation are energetic synoptic scale westerly wind bursts which are often associated with tropical cyclone formation [Keen, 1988] and the westerly phase of intraseasonal oscillations [Sui and Lau, 1992]. Seasonally, wind bursts tend to occur most frequently during November–April. They also tend to develop more frequently prior to and during El Niño–Southern Oscillation (ENSO) events [Luther et al., 1983; Harrison and Giese, 1991], suggesting a possible dynamical coupling between synoptic-scale wind forcing and the low-frequency evolution of the coupled ocean-atmosphere system. The mechanistic connection invoked between wind burst forcing and the ENSO phenomenon involves the excitation of Kelvin waves which advectively alter the eastern Pacific sea surface temperature field [Keen,

1982; Harrison and Schopf, 1984] and the local oceanic response which alters the heat content of the western Pacific warm pool [Lukas and Lindstrom, 1991].

Although there is ample evidence for the excitation of equatorial Kelvin waves in response to the wind burst forcing prior to and during the 1986–1987 ENSO [Miller et al., 1988; McPhaden et al., 1988; McPhaden and Hayes, 1990], documentation of the regional response in the western Pacific to wind burst forcing has been mostly piecemeal and based on studies of individual data sets from differing time periods. For example, Hisard et al. [1970] were the first to observe a reversal of zonal currents in the deep 100-m surface layer of the western Pacific from shipboard current profiles in response to a 10-day westerly episode in March 1967. These changes observed in vertical structure though were based on only two meridional sections separated by 1 month. Later, Burkov et al. [1976] described the complicated vertical structure of zonal currents in the upper 100 m from mooring deployments of 1–5 days' duration at 0°, 165°E. Their time series were too short, however, to examine the relationship of the current variability to local wind forcing. McPhaden et al. [1988] used longer moored time series data of winds and currents at 0°, 165°E, to describe the response to a 10-day westerly wind burst in May 1986. The rapid eastward acceleration of the surface layer in response to this wind burst was well documented, but from only the equatorial site and only from four depths in the upper 200 m. A single meridional section of acoustic Doppler current profiler (ADCP) data in December 1986 indicated a latitudinal half width of about 2° for an intense equatorially trapped westerly wind-driven jet [Delcroix et al., 1992], the temporal evolution of which was described by McPhaden et al. [1990a].

US/PRC Bilateral Cruise #7
Xiangyanghong #14
Guangzhou, PRC – Guam
12 October – 26 November 1989

● ATLAS Mooring   ● Island Wind
■ CM Mooring   × Drifting Thermistor
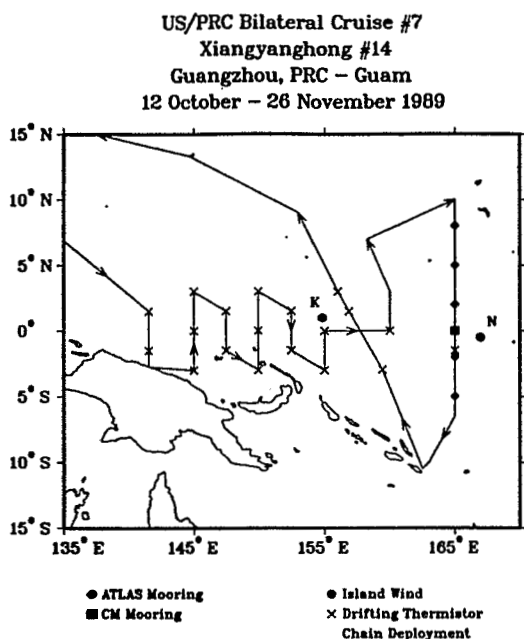   Chain Deployment

Fig. 1. Locations of the ATLAS moorings, current meter moor-ing, and island wind stations used in this study. The island wind stations are Kapingamarangi (K) and Nauru (N). Also shown is the cruise track of the *Xiangyanghong #14* which conducted the sev-enth cruise of the U.S.-PRC Bilateral Air-Sea Interaction Program between October 12 and November 26, 1989. Deployment sites of drifting thermistor chains are superimposed on this cruise track.

McPhaden and Hayes [1991] described the upper ocean thermal response to wind burst forcing during the 1986–1987 ENSO, highlighting the role of evaporative cooling in chang-ing SST and upper layer heat content in the vicinity of 0°, 165°E.

In the late 1980s, mooring and drifting buoy deployments increased in the western equatorial Pacific as part of the Tropical Ocean–Global Atmosphere (TOGA) observing ar-ray, and new kinds of instrumentation such as moored conductivity and temperature recorders were introduced. Fortuitously, in late 1989 and early 1990 a series of strong westerly wind bursts occurred at a time when two shipboard surveys were under way and several new instrument systems were being deployed. The purpose of this paper is to provide a summary of these data, which offer a unique description of the ocean's response to wind burst in the western equatorial Pacific.

The remainder of this paper is organized as follows. Section 2 summarizes the data sets used, with details rele-gated to an appendix. Section 3 provides a description of the space and time scales of the wind forcing during November 1989 to January 1980, while section 4 describes the spatial and temporal evolution of upper ocean currents and hydrog-raphy in response to this wind forcing. We conclude in section 5 with a brief summary and discussion of results.

2. Data

The oceanic data utilized in this study derive from a number of sources. These include an ATLAS and current meter mooring array, and island wind stations shown in Figure 1. In addition, 21 drifting thermistor chains were deployed along the cruise track of the R/V *Xiangyanghong*

#14, which conducted the seventh cruise of the United States–People's Republic of China (U.S.-PRC) Bilateral Air-Sea Interaction Program in October–November 1989. Acoustic Doppler current profiler data were collected on leg 2 (Ponape to Guam), and a conductivity-temperature-depth (CTD) section was made between 10°N, 165°E, and 10°S, 162°E. In December 1989, SURTROPAC-13 was conducted by the French R/V *Le Suroit* along 165°E between 16°S and 8°N, during which CTD and Aanderaa profiling current meter measurements were made. Finally, in November–December 1989, the region between 10°N and 10°S west of the date line was populated by approximately 20–30 circula-tion drifters as part of the Pan-Pacific drifters experiment. These instrument systems and data types are discussed more thoroughly in the appendix.

3. Wind Forcing

Following the 1986–1987 ENSO, winds were anomalously easterly by 1–3 m s^{-1} for nearly 2 years over much of the western equatorial Pacific between 135°E and the date line [*Climate Analysis Center*, 1991]. Synoptic scale westerly wind events occurred infrequently and were generally of weak amplitude and short duration. Then in November 1989 a sequence of much stronger and longer lasting westerly bursts developed, the first of which is evident in an opera-tional surface wind analysis on November 27, 1989 (Figure 2). Westerlies with typical speeds of 5–10 m s^{-1} were apparent along the equator from 130°E to nearly the date line on this day. These westerlies, as well as related northerly and southerly flows along the equator, were associated with a cyclonic circulation centered near 9°N, 145°E, which later developed into supertyphoon Irma. Winds along Irma's storm track eventually reached speeds in excess of 70 m s^{-1} as she migrated northwestward before weakening in the Philippine Sea.

Between November 1989 and March 1990, five or six episodes of equatorial westerlies occurred similar to those associated with Irma. They typically lasted for 10–15 days, with maximum amplitudes of 5–10 m s^{-1}. The timing and amplitudes of these westerlies are accurately determined from moored and island time series measurements, revealing a complicated spatial structure to the wind field. For exam-ple, the strong November event was preceded at 155°E by several shorter-duration westerly episodes in October which were less pronounced at 165°E (Figure 3a). Westerly winds also appeared earlier and lasted longer at 155°E than at 165°E during the strong wind burst that began in November. Conversely, east of the date line at 170°W where strong trade winds normally prevail, winds were almost always easterly with the exception of brief periods of westerlies in January and February 1990. Along 165°E, the strong November wind burst appeared to develop initially at the northernmost mooring site (8°N) and then slowly migrate southward to-ward the equator (Figure 3b). Subsequent westerly events were less pronounced north of the equator, whereas they tended to be stronger and persist longer south of the equator. The shift toward persistent easterlies in the northern hemi-sphere during December–March was part of the normal seasonal cycle, as was the tendency for westerlies early in the year at 5°S. However, synoptic time scale westerly anomalies were still evident at 5°N and 8°N during Decem-ber–March; also the westerly winds in the southern hemi-
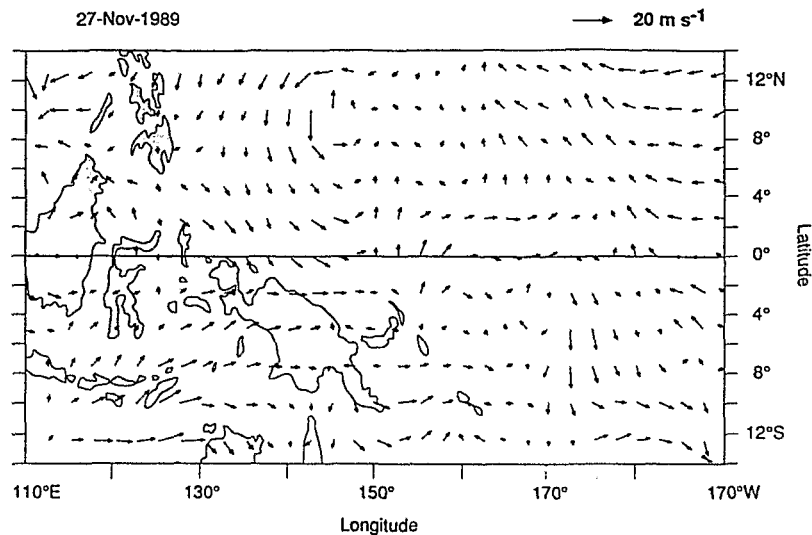
27-Nov-1989   ⟶ 20 m s⁻¹

Fig. 2. Winds at 19.5 m height for 0000UT on November 27, 1989, from the Fleet Numerical Oceanography Center gridded analysis.

sphere at this time were more episodic and much stronger than climatology.

4. OCEANIC RESPONSE

4.1. Current Meter Mooring Measurements

The rapid response of the surface layer temperature and zonal velocity field to westerly wind forcing are evident in time series collected from the 0°, 165°E, current meter mooring. Prior to the initial wind burst in mid-November 1989, the surface layer was weakly stratified with a 1°C vertical gradient over the upper 100 m (Figures 4 and 5). The South Equatorial Current (SEC) flowed westward at about 20 cm s⁻¹ near the surface, and the Equatorial Undercurrent (EUC), centered around 200-m depth in the thermocline, flowed eastward at speeds of about 40 cm s⁻¹. A secondary eastward maximum of 20 cm s⁻¹ was observed between the SEC and EUC in the weakly stratified region near 100-m depth. The vertical structure of temperature and zonal currents in early November 1989 was reminiscent of that first described by *Hisard et al.* [1970].

Prior to the onset of westerlies in November 1989, there was tendency toward decreasing thermal stratification in the upper 100 m at 0°, 165°E. This tendency accelerated shortly after the winds switched to westerly on November 19, and within a week the upper 100 m became isothermal to within about 0.1°C (Figures 4 and 5). A similar rapid homogenization of temperature in the upper 100 m at 0°, 165°E was observed in association with the May 1986 westerly wind burst [*McPhaden et al.*, 1988]. The surface layer remained isothermal to within 0.2°–0.3°C afterwards, except during periods of low wind speed when sea surface temperature (SST) rose by 0.5°C or more and the upper 10 m tended to restratify (e.g., in early December and in early January). The inverse relationship between wind speeds and SST was noted previously by *McPhaden and Hayes* [1991], who suggested an important role for evaporative cooling in the SST balance on wind burst time scales. It is also possible that reduced incoming shortwave radiation contributed to the inverse relationship between wind burst forcing and

SST, since wind bursts are associated with enhanced cloudiness and convection along the equator [*Lander and Morrissey*, 1988; *Nitta and Motoki*, 1987].

We also note that the warmest temperatures were not always found at the surface. For example, SST dropped about 0.3°C in mid-December following peak wind speeds greater than 8 m s⁻¹ associated with the December wind burst; temperatures below 50 m, on the other hand, changed little at this time. Thus an inversion developed with surface temperatures colder than temperatures at 50- to 100-m depth. This inversion (and others in the record, such as at the end of January) were supported by vertical buoyancy gradients determined mainly by low salinities (34.1–34.4 psu) near the surface and higher salinities (34.6–35.1 psu) at 100 m (Figure 6).

In contrast to the surface temperatures, which locally tended to fall in response to strong westerly wind forcing, temperatures at a depth of 150 m in the upper thermocline initially increased after the onset of westerlies (Figure 4d). The 26°C isotherm for example deepened by about 20–30 m from mid to late November, as one might expect from either meridional Ekman convergence or a convergence of flow in the zonal direction (see below). Subsequent to this initial deepening, however, isotherms in the 18°–28°C range gradually shoaled, and only deeper isotherms (e.g., the 14°C isotherm) appeared to be depressed in response to westerly wind forcing in December and January.

Zonal currents in the surface layer underwent dramatic changes with the onset of westerly winds in November 1989. At 10-m depth, the currents accelerated rapidly to the east, reversed, and reached speeds over 100 cm s⁻¹ in 1 week (Figure 4b). Zonal currents at 50-m and 100-m depth also accelerated eastward, although at a slower rate and delayed by a few days relative to the 10-m currents (Figure 4c). Conversely, flow at 150-m depth accelerated westward after the onset of strong westerlies, reaching speeds of more than 40 cm s⁻¹ by early December (Figure 4c). This westward counterflow separated the eastward flow near the surface from the Equatorial Undercurrent in the thermocline. Changes in undercurrent speeds were generally smaller than
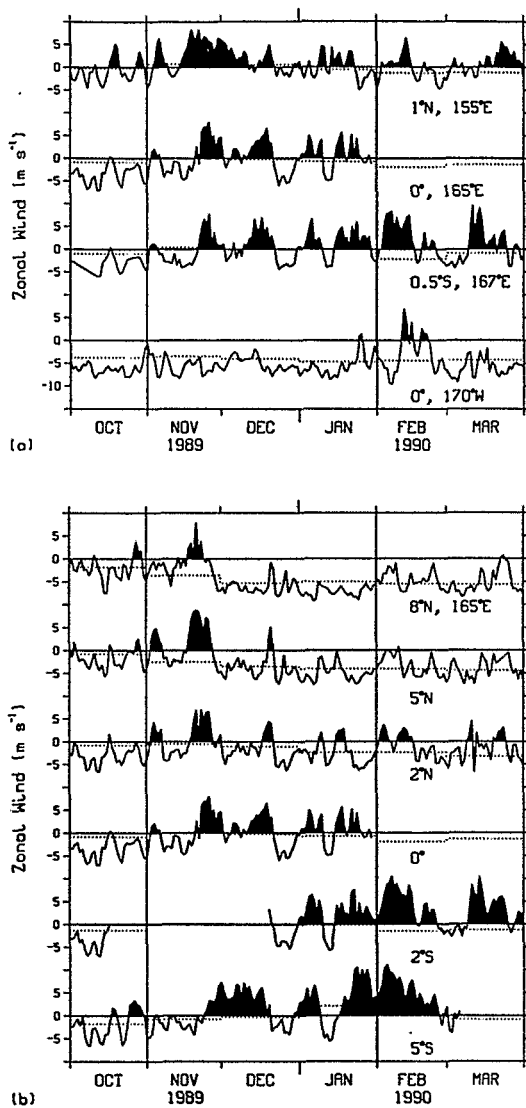
Fig. 3. Daily averages of the surface zonal winds (a) near the equator between 155°E and 170°W and (b) along 165°E between 5°S and 8°N. Data are from the array of ATLAS moorings, island wind stations, and the current meter mooring at 0°, 165°E. Dotted lines show the Wyrtki and Meyers [1975] climatology. Vertical bars bracket the period November 1989 to January 1990.

those near the surface. However, the undercurrent decelerated to less than 50% of its original speed before the onset of westerlies, reaching a minimum of less than 20 cm s⁻¹ by early December.

Zonal currents responded to westerly wind forcing in December and January much as they responded in November. In each case, surface currents accelerated eastward, and westward counterflow could be found below the surface eastward jet. For the record as a whole, the surface winds lead the 10-m currents by 1 day based on cross-correlation analysis of the time series in Figures 4a and 4b. However, there were also notable differences in the current responses during November–January. For example, the maximum eastward current speeds achieved in December and January at 10-m depth were smaller than those in November, consistent with the weaker local wind forcing. There also appeared to be subtle differences in the timing of the current response relative to the local winds, with more of a lag between 10-m

currents and local winds in December and January than in November (compare Figures 4a and 4b). In addition, the reversing jet structure was confined to a shallower range of depths as the thermocline shoaled in January. Finally, although the speed of the undercurrent decreased significantly following the November wind burst, similar decelerations were not observed in December and January. On the contrary, the undercurrent accelerated over the latter half of the record, relatively unaffected by the occurrence of local westerly winds.

4.2. Profiling Current Meter Data

The latitudinal width of the eastward surface jets was about 400–600 km, based on a comparison of profiling current meter sections made in November and December 1989 (Figures 7 and 8). The first two of these sections (Figures 7a and 7b) were made in November with a ship-mounted ADCP during U.S.-PRC 7. These sections were separated by 8° of longitude at the equator, so that some of the differences between them may be related to spatial variations in the response to wind burst forcing. However, the zonal scales were larger than 8° for surface layer zonal velocities (section 4.4), so that it is reasonable to interpret
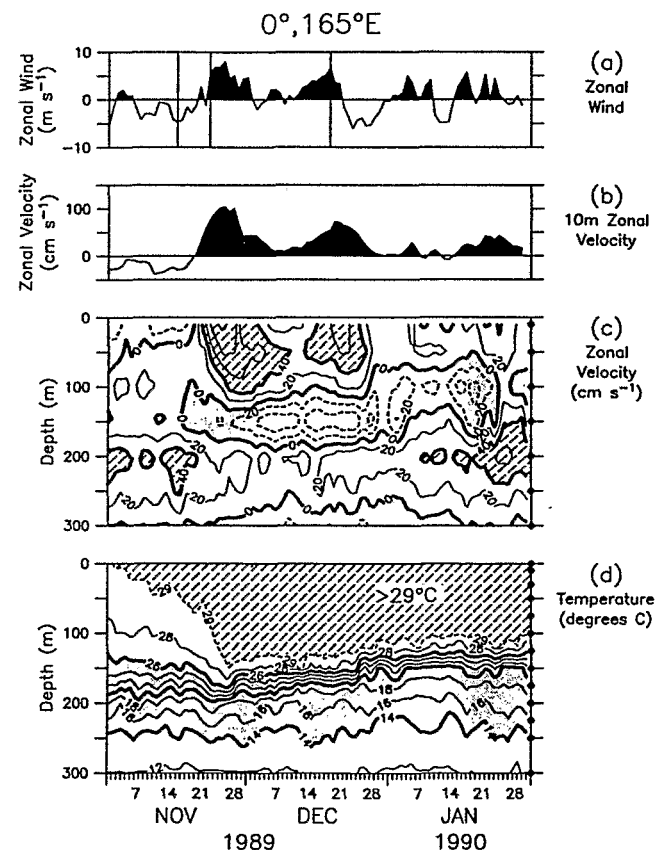

Fig. 4. Daily averages of (a) zonal wind, (b) 10-m zonal currents, (c) 10- to 300-m zonal currents and (d) 0- to 300-m temperatures from the current meter mooring at 0°, 165°E, for November 1989 to January 1990. The contour interval in Figure 4c is 20 cm s⁻¹ with westward flow shaded, and eastward flow >40 cm s⁻¹ hatched. The contour interval in Figure 4d is 2°C, except for the 29°C isotherm which is indicated by a dashed contour. Instrument depths are indicated on the right sides of Figures 4c and 4d. Vertical bars in Figure 4a indicate equatorial crossing of the Xiangyanghong #14 in November, and the Le Suroit in December.
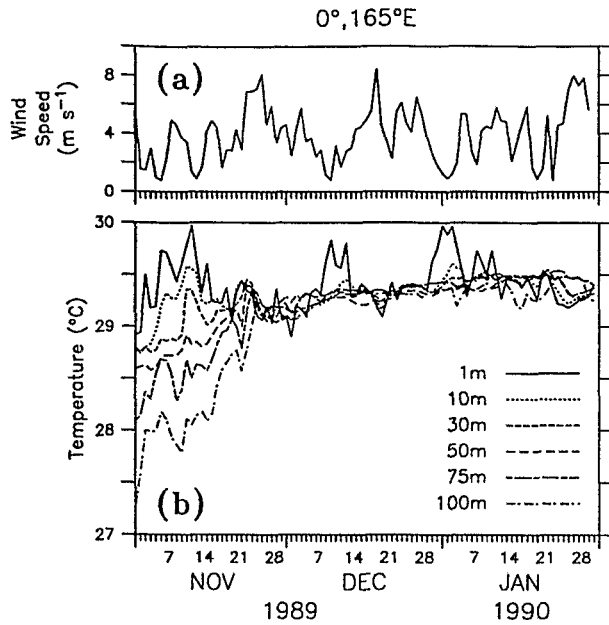
0°,165°E

Fig. 5. Daily averages of (a) wind speed and (b) temperature in the upper 100 m at 0°, 165°E.

the differences between Figures 7a and 7b in the upper 150 m near the equator primarily in terms of time variations.

Prior to the onset of strong westerly winds at 165°E, the South Equatorial Current flowed westward at speeds of 10–40 cm s^{-1} in the upper 160–180 m between 3°N and 4°S (Figures 7a and 8a). Embedded in the SEC was a weak eastward flow centered near 100-m depth between 1°N and
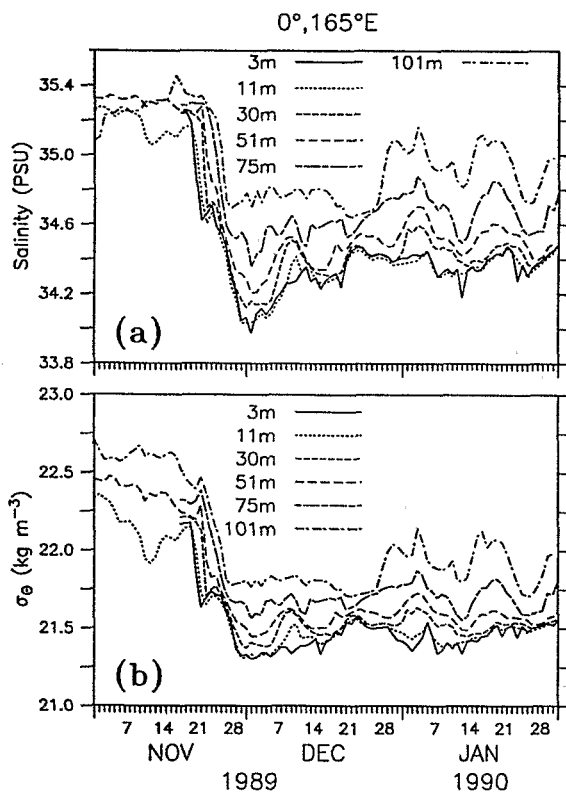
0°,165°E

Fig. 6. Daily averages of (a) salinity and (b) density (σ_θ) in the upper 101 m at 0°, 165°E.
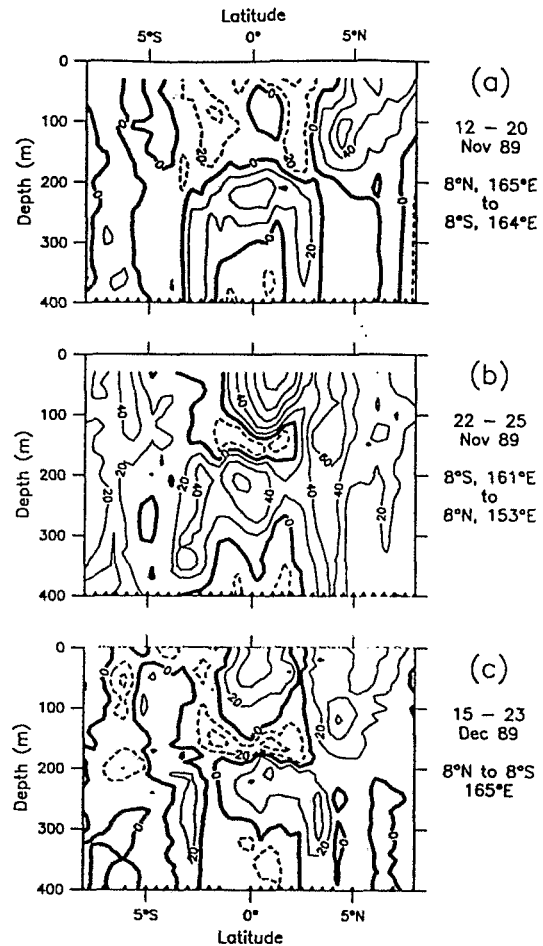

Fig. 7. Meridional sections of zonal velocity; (a) ADCP section between 8°N, 165°E, and 8°S, 164°E, for November 12–20, 1989; (b) ADCP section between 8°S, 161°E, and 8°N, 153°E, for November 22–25, 1989; and (c) Aanderaa profiling current meter section between 8°S and 8°N, 165°E, for December 15–23, 1989. The contour interval is 20 cm s^{-1} with westward flow shaded. Triangles along the latitude axis indicate the 0.5 resolution of the gridded ADCP data set in Figures 7a and 7b and the station spacing for the Aanderaa profiler data in Figure 7c.

1°S. This feature was noted earlier in discussion of the mooring data (Figure 4c). The eastward North Equatorial Countercurrent (NECC) can be seen to the north of the SEC, with a 70 cm s^{-1} subsurface maximum centered near 100-m depth at 4.5°N. A weaker eastward South Equatorial Countercurrent (SECC) with speed ≤20 cm s^{-1} was located between 6° and 8°S. Below the SEC, the Equatorial Undercurrent flowed eastward in the thermocline between 2°N and 2°S with maximum speeds of ≤40 cm s^{-1}. Deeper still, between 300- and 400-m depth, was the westward Equatorial Intermediate Current [Delcroix and Henin, 1988] which was flanked by the North and South Equatorial Subsurface countercurrent centered at 2.5°N and 2.5°S, respectively.

Seven days after the Xiangyanghong #14 crossed the equator heading south along 165°E, it recrossed the equator heading north at 157°E (Figure 1). By this time the winds had switched from easterly to westerly and had reached near maximum speeds. Consistent with the mooring data, the zonal current structures in the upper 150 m underwent a remarkable transformation during this interval (Figures 7b and 8). An eastward jet with maximum speeds of over 100
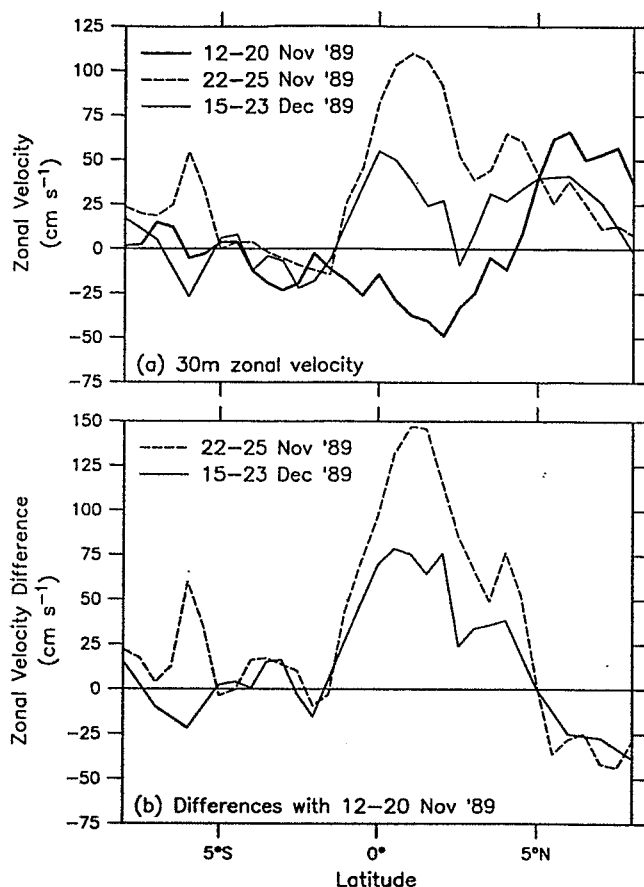
Fig. 8. (a) Zonal velocity as a function of latitude at 30-m depth based on shipboard profiling current meter data for November 12–20, 1989 (heavy solid line), November 22–25, 1989 (dashed line), and December 15–23, 1989 (light solid line). (b) Zonal velocity differences at 30 m relative to the November 12–20, 1989, transect.

cm s^{-1} replaced the westward SEC in the upper 100 m between 1.5°S and 2.5°N. Simultaneously, westward flow centered near 150-m depth intensified from 2°N to 2°S. The eastward surface jet was more strongly developed north of the equator, perhaps because westerlies were stronger north of the equator at this time (Figure 3b), or because of meandering associated with the excitation of wave transients (see section 5).

Circulation changes also occurred at higher latitudes between the two equatorial ADCP transects on U.S.-PRC 7. For example, in the vicinity of the NECC, eastward flow intensified by as much as 50 cm s^{-1} between about 3° and 5°N and weakened by 25–35 cm s^{-1} between 6°N and 8°N. Similarly, the SECC broadened and substantially intensified from mid to late November. These changes, though smaller than the largest changes within 2° of the equator, were nonetheless significant and probably related to effects of wind burst forcing which extended over a wide range of latitudes (Figures 2 and 3).

We estimated the volume transports in the upper 150 m of Figures 7a and 7b by integrating in latitude and depth using the trapezoidal rule. For this calculation, zonal velocity was approximated as a constant between the surface and 20 m, which was the shallowest depth sampled. Two calculations were done, one for the latitudinal range 1.5°S to 2.5°N, and a second for the latitudinal range 1.5°S to 5°N. Although the

zonal velocity switched from westward to eastward between 1.5° and 5°N in mid-November (Figure 8b), the relative eastward velocity minimum near 3°N appears to define the boundary between the NECC and the equatorial jet. The dynamics of velocity change in the two currents may to be different, suggesting that a distinction be made in estimating the transport variations over the full range of latitudes. The results (Table 1) indicate that volume transport between 1.5°S and 2.5°N was 11.1 Sv (1 Sv = 10^6 m^3 s^{-1}) to the west prior to the onset of westerlies in mid-November and 28.7 Sv to the east after the onset of westerlies. For the latitude range 1.5°S to 5°N, the corresponding transports were 5.3 Sv to the west and 50.8 Sv to the east. Thus the change in volume transport in response to the westerly wind event in November 1989 was 40–56 Sv in about 1 week, depending on the range of latitudes considered. For perspective, these transport changes are larger than the mean transport of the SEC (38 Sv) between 10°S and 4°N, the mean transport of the EUC (20 Sv), and the mean transport of NECC (27 Sv) along 165°E [Delcroix et al., 1987].

The R/V Le Suroit conducted SURTROPAC 13 along 165°E about 1 month after U.S.-PRC 7. Between these two cruises, the westerlies had abated in early December, and the surface eastward jet decelerated. However, by the time the Le Suroit crossed the equator on December 18, westerly winds had reintensified along 165°E and the surface currents were once again accelerating toward the east (Figure 4b). The structure of the zonal currents on this cruise was similar to that observed on U.S.-PRC 7 in late November (Figures 7c and 8a). An eastward jet was again observed between about 1.5°N and 2.5°S in the upper 100 m and was separated from the EUC in the thermocline by a westward counterflow centered at 150 m. Similarly, stronger eastward flow relative to that in mid-November was observed between 3°N and 5°N in the vicinity of the NECC, and weaker eastward flow was observed north of 5°N (Figure 8b). However, unlike the eastward equatorial jet observed on U.S.-PRC 7, the maximum eastward velocity on SURTROPAC 13 was located at the equator rather than at 1°N, and the maximum speed (about 60 cm s^{-1}) was roughly half that of the jet in late November. Net volume transport was 7.9 Sv to the east between 1.5°S and 2.5°S and 19.5 Sv to the east between 1.5°S and 5°N during SURTROPAC 13 (Table 1). These transports, though substantially lower than those during the first pronounced wind burst in late November, were still 19–25 Sv more eastward than those observed prior to the onset of westerlies.

4.3. Shipboard Hydrographic Measurements

Changes in the water mass structure on the meridional plane associated with these wind driven zonal jets are

TABLE 1. Zonal Volume Transport Between 0 and 150 m for Velocity Transects Along 165°E (November 12–20 and December 15–23, 1989) and Along 163°–151°E (November 22–25, 1989)

	Transport, Sv	
	1.5°S to 2.5°N	1.5°S to 5°N
November 12–20	−11.1	−5.3
November 22–25	28.7	50.8
December 15–23	7.9	19.5

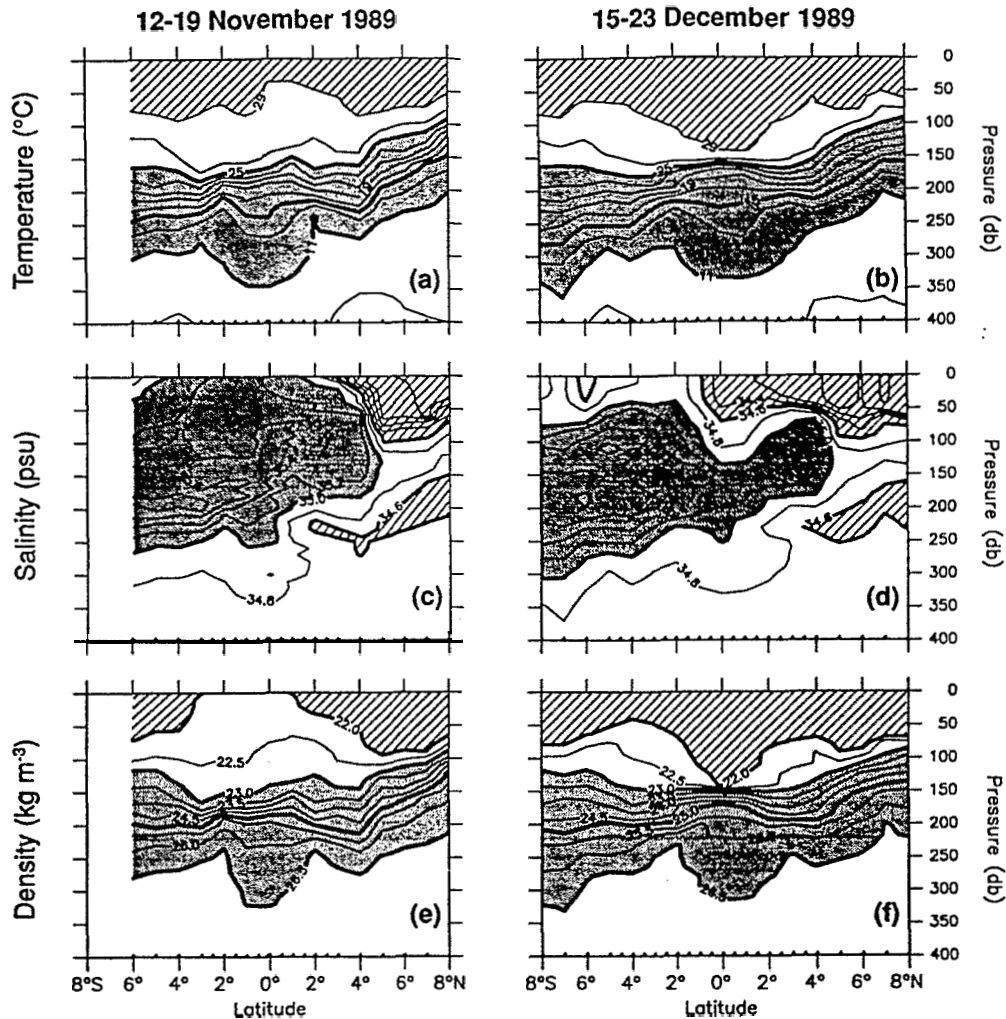Positive transport is toward the east; 1 Sv = 10^6 m^3 s^{-1}.

Fig. 9. Temperature, salinity, and density along 165°E in November 1989 and December 1989. Station spacing is indicated by small triangles along the latitude axis. (a) November temperature, (b) December temperature, (c) November salinity, (d) December salinity, (e) November density (σ_t), (f) December density (σ_t).

evident in Figure 9a. Prior to the onset of westerlies in November 1989, there was weak thermal stratification in the upper 100–150 m, below which the more strongly stratified thermocline was found (Figure 9a). The thermocline weakened near the equator owing to the presence of geostrophically balanced vertical shear associated with the SEC-EUC system; the thermocline also sloped upward north of 4°N to geostrophically balance the eastward NECC. Salinity, which is a better indicator of equatorial upwelling than temperature in the western Pacific [Donguy and Dessier, 1983], was a maximum at the surface with values greater than 35.3 psu at about 1.5°S (Figure 9c). A sharp meridional salinity gradient at 2°–4°N separated this surface maximum from low-salinity waters (<34.0 psu) in the vicinity of the NECC. These low-salinity surface waters were associated with the high rainfall rates of the intertropical convergence zone [Delcroix and Henin, 1991]. In the thermocline, a high-salinity tongue of southern hemisphere subtropical water (>35.0 psu) penetrated to 4°N, and a tongue of low-salinity northern hemisphere intermediate water (<34.6 psu) was evident at depths of 150–250 m poleward of 1°N. The density field (Figure 9e) was strongly influenced by salinity near the surface, but mainly determined by temperature in the thermocline.

Isopycnals in the upper 100 m sloped upward toward the equator in both hemispheres between 4°N and 4°S in mid-November 1989, indicative of Ekman divergence and equatorial upwelling associated with easterly wind forcing.

After the onset of westerlies, significant changes took place in the temperature, salinity, and density fields in the upper 150 m within a few degrees of the equator (Figures 9b, 9d, and 9f). In mid-December, shallow isotherms and isopycnals sloped down toward the equator between about 4°N and 4°S (Figures 9b and 9f), suggestive of downwelling in response to Ekman convergence. Also, the sharp salinity front centered near 3°N in November was displaced to 1°S, and the surface salinity maximum at 1.5°S was replaced by near-equatorial salinity minimum. Examination of Figure 6a shows that this frontal displacement occurred primarily in late November, when, for example, salinity in the upper 11 m dropped from 35.2 psu on November 19 to 34.0 on December 1 at 0°, 165°E. Assuming that these salinity changes were due only to meridional advection and that the waters with salinity of 34.0–34.6 psu were initially found at the surface between 3° and 4°N along 165°E (Figure 9c), we infer an average southward velocity of 40–50 cm s^{-1} north of the equator for the latter part of November. These velocities
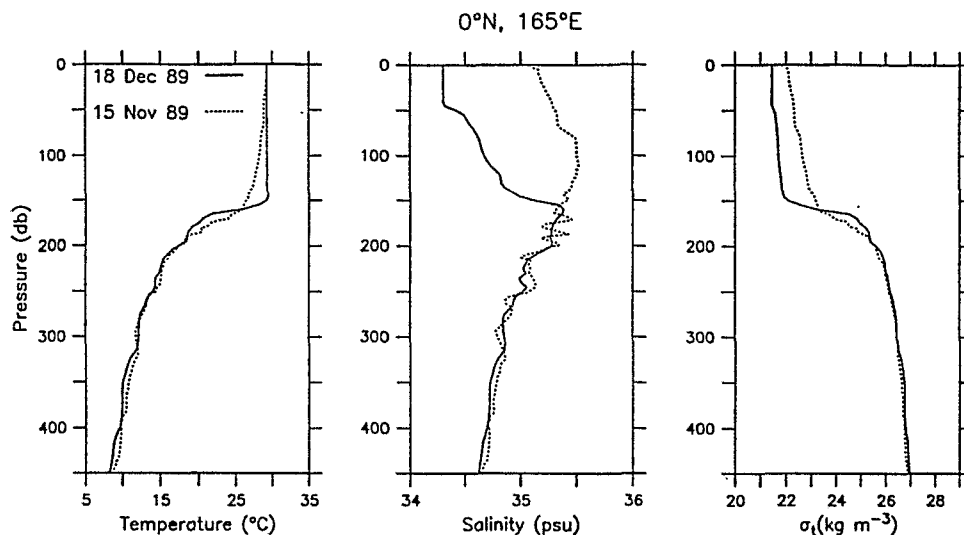
0°N, 165°E

Fig. 10. Temperature, salinity, and density (σ_t) profiles from CTD stations on November 15, 1989, at 0°01'S, 165°01'E (dashed) and December 18, 1989, at 0°00', 165°00'E (solid).

are roughly comparable to southward velocities of 20–50 cm s^{-1} observed from circulation drifters a few degrees north of the equator near 165°E as discussed in section 4.4.

Equatorial CTD profiles (Figure 10) emphasize the relative uniformity in temperature in the upper 150 m after the onset of westerlies and also the central role that salinity played in determining density variations near the surface. Specifically, the density mixed layer in December 1989 was significantly shallower than the temperature mixed layer because of the existence of a sharp halocline or "barrier layer" [*Lukas and Lindstrom*, 1991] at 50–60 m. Such shallow haloclines may have been instrumental in thermally insulating the near surface from the thermocline [e.g., *McPhaden and Hayes*, 1991] and may explain why high winds in mid-December and late January were associated with temperature inversions in the upper 100 m (see Figure 5). It is likely that turbulence generated by these winds was unable to erode the near-surface halocline and that enhanced evaporative cooling and/or reduced insolation caused a drop in SST that could not completely mix down to 100 m.

The shallow density changes evident in Figure 9 are consistent with the expected geostrophic balance of the near surface zonal currents along 165°E [*Picaut et al.*, 1989, 1990]. Specifically, the upward sloping 22.0 kg m^{-3} isopycnals in Figure 9e were associated with predominantly westward flow in a geostrophically balanced SEC, and the same downward sloping isopycnals in Figure 9f were associated with a strong near-surface eastward geostrophic jet. A change from westward to eastward near-surface zonal flow along the equator also requires that the upper equatorial thermocline sharpen to maintain a density field in thermal wind balance with the vertical shear. Hence the sharper thermocline and pycnocline between 150 m and 200 m evident in Figure 10 is not a priori evidence for turbulent entrainment from the thermocline as might be inferred from simple one-dimensional mixed layer models. Rather, the sharper thermocline and pycnocline may result from the completely adiabatic dynamical process of geostrophic adjustment near the equator. This interpretation is supported by the existence of shallow haloclines which, as was noted

above, tend to isolate the thermocline from the effects of near-surface mixing processes.

Dynamic height of the sea surface relative to 1000 dbar along 165°E (Figure 11) shows that the equatorial trough was located at about 1°N and the equatorial ridge was located at 4°N in mid-November 1989 when easterly trade winds prevailed. One month later after the onset of westerlies, dynamic heights rose by 10–12 dyn cm between 1°S and 3°N, and fell by a few dynamic centimeters poleward of 3°N. The equatorial trough near 1°N was filled in, and sea level sloped downward almost continuously from the equator to 8°N. The near-equatorial changes in dynamic height were consistent with a switch from easterlies in November which favor Ekman divergence and upwelling, to westerlies in December which favor Ekman convergence and downwelling. The change in meridional slope of the sea surface near the equator was also indicative of the reversal in geostrophically balanced surface currents between November and December as discussed above.

4.4. Drifting Buoy Measurements

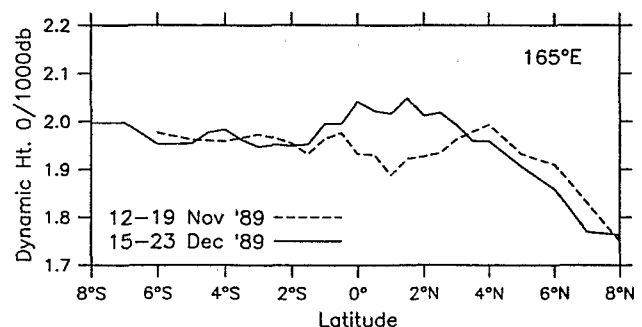Trajectories of circulation drifters drogued at 15-m depth (Figure 12) indicate that the eastward jet extended over

Fig. 11. Dynamic height of the sea surface relative to 1000 dbar along 165°E from U.S.-PRC 7 in November 1989 (dashed) and SURTROPAC 13 in December 1989 (solid).

Drogued Circulation Drifters
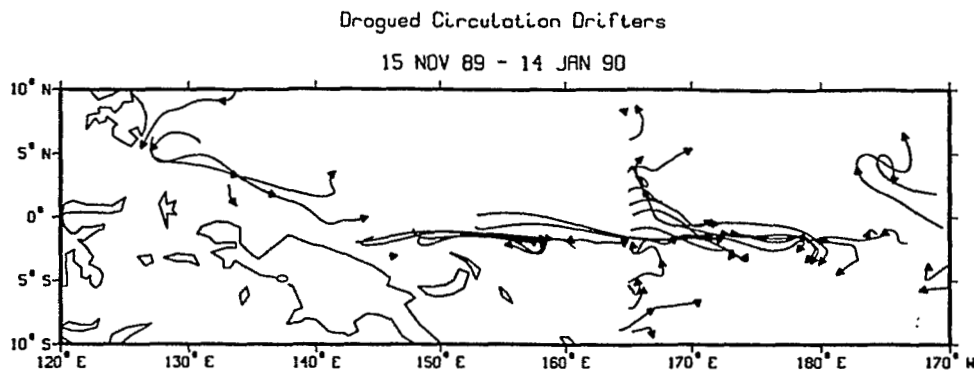
15 NOV 89 - 14 JAN 90

Fig. 12. Trajectories of circulation drifters between November 15, 1989, and January 14, 1989. Trajectories have been smoothed with a 15-day Hanning filter. All drifters are drogued at 15-m depth. Arrowheads are plotted every 30 days, counting backward from the last day of data available.

about 40° of longitude (140°E to 180°) from November 1989 to January 1990. This jet did not penetrate much past the date line, east of which westward flow in the SEC was evident. Moreover, consistent with the shipboard ADCP and hydrographic data, the jet was narrowly confined to within a few degrees of the equator. Flow was generally meridionally convergent, as would be expected during episodes of strong westerly winds; i.e., buoys once entrained into the eastward jet did not deviate far from the equator (except at its eastern terminus in January 1990). Ekman convergence was particularly noticeable in the meridional array of drifters deployed from the *Le Suroit* along 165°E when buoys launched within several degrees of the equator in both hemispheres migrated equatorward. One can also see convergence toward the equator west of 140°E from a drifter which is entrained into the jet from the region of the Mindanao Current.

A dramatic example of the changes in horizontal flow structure that took place after the onset of the first large westerly wind burst in November 1989 can be seen in Figure 13. In mid-November the westward SEC extended over most of the region between 170°W and 135°E near the equator, although there was an area of weak eastward flow between 150°E and 160°E at this time as well (Figure 13a). Westward speeds in the SEC ranged from less than 10 cm s^{-1} to over 100 cm s^{-1}, but typically they fell between 30 and 50 cm s^{-1} for the drogued drifters and 10-m current meter measurements. Winds were predominantly easterly at

this time, although incipient westerlies developed in the area of weak eastward surface flow between 150°E and 160°E (see the Kapingamarangi (1°N, 155°E) record in Figure 3a). These weak eastward currents were the first signs of the jet that became more fully developed in response to intensified and widespread westerly wind forcing. Indeed, 10 days later, flow almost everywhere west of the date line had an eastward component, with largest velocities between about 2°N and 2°S (Figure 13b). Maximum zonal flow of nearly 140 cm s^{-1} occurred near the equator between 155°E and 160°E. Consistent with Figure 12, the flow reversal was evident over about 40° of longitude but did not penetrate past the date line. Superimposed on the eastward jet was a broad-scale meander with a tendency for northward flow along the equator at between 145°–155°E, and southward flow along the equator at 155°–165°E.

We estimated the magnitude of horizontal convergence in the surface layer near 0°, 165°E, using the drogued circulation drifters shown in Figure 13b for November 27–29. Ekman convergence in the meridional direction was found to be about 1.1×10^{-6} s^{-1} based on drifter velocities from near 2°N and 3°S, 165°E. A similar calculation for convergence in the zonal direction using drifters near the equator between 157°E and 179°W resulted in an estimate of 0.7×10^{-6} s^{-1}, which was about 60% of the estimate of meridional convergence. Assuming for the sake of argument that horizontal velocities were uniform in the upper 15 m, these conver-
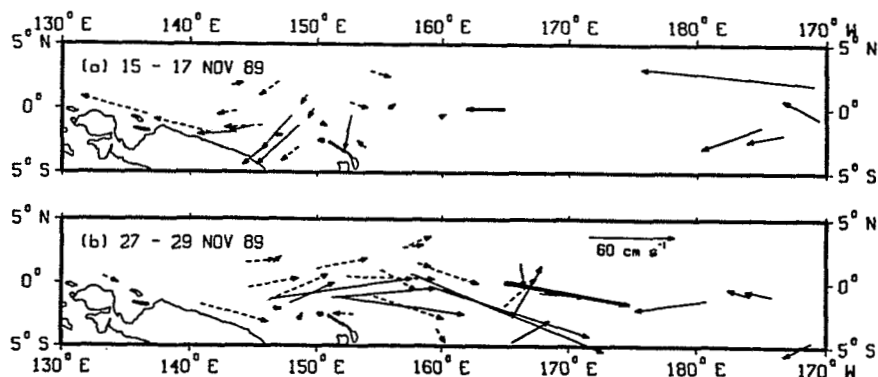

Fig. 13. Composite chart of velocity vectors for circulation drifters (solid arrows), moored current meter at 10-m depth (heavy solid arrow), and drifting thermistor chains (dashed arrows) for (a) November 15–17, 1989, and (b) November 27–29, 1989. Vectors are 3-day averages, with the tail of the arrow located at the 3-day mean of individual buoy positions.
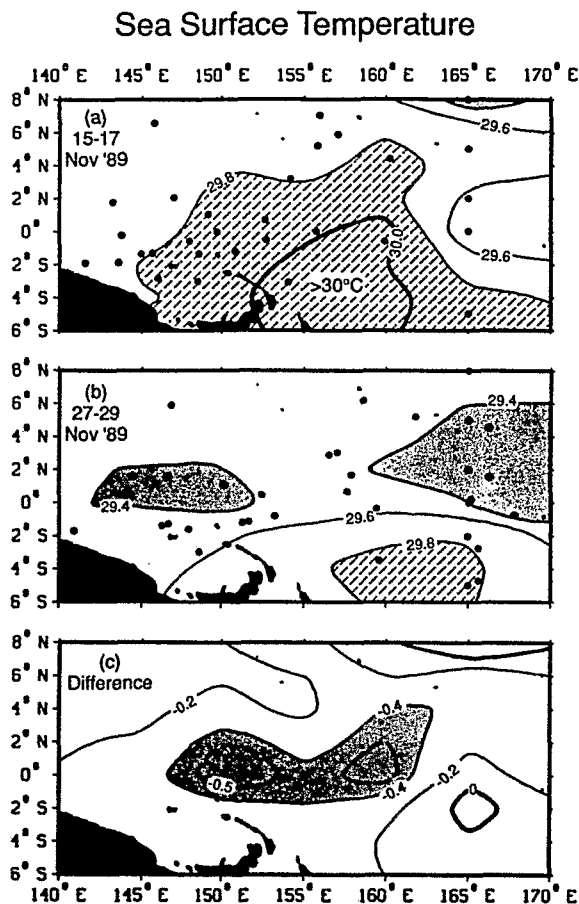
Sea Surface Temperature

Fig. 14. Sea surface temperature maps for (a) November 15–17, 1989, and (b) November 27–29, 1989, with (c) the difference field (November 27–29 minus November 15–17). Data in Figures 14c and 14b are averaged over the same 3-day intervals as in Figure 13 using drifting buoy and mooring data; data distribution (3-day mean positions) is indicated by dots. Data have been objectively analyzed using a Laplacian gridding routine. Spatial gradients have been weighted anisotropically, producing a field effectively smoothed over 2° of latitude and 5° of longitude. Hatching in Figures 14a and 14b indicates water warmer than 29.8°C, and gray shading indicates water colder than 29.4°C. Shading in Figure 14c indicates differences ≤ −0.4°C. Contour intervals are 0.2°C, except for the 0.5°C contour in Figure 14c, which is dashed.

gence estimates imply downwelling at drogue depth of 2.8 × 10^{-5} m s^{-1}, or 2.4 m d^{-1}. Both the sign and magnitude of this vertical velocity estimate are consistent with the plunging of the 29°C isotherm in late November 1989 at 0°, 165°E (Figure 4d) and suggest that warming in the surface layer at depths below 15 m at this time was due at least in part to vertical advection. Equatorial downwelling is also consistent with the 20- to 30-m depression of the thermocline and the 10 dyn cm elevation in sea level along 165°E discussed earlier.

Drifter data (in combination with mooring data) were used to map sea surface temperature changes associated with the evolution of the surface velocity field. Figure 14, for example, shows the SST field between 6°S and 8°N, 140°–170°E, for the same times as the synoptic circulation charts in Figure 13. In mid-November 1989 (Figure 14a), SSTs were typically between 29.6°C and 30.0°C with the warmest water at 150°–160°E south of the equator. Evidence for penetration of the equatorial cold tongue into the western Pacific can be seen near 165°E, coincident with upwelling favorable east-

erly wind forcing along this meridian. Ten days later, after the onset of westerlies (Figure 14b), the warmest water to be found was 29.8°C at 2°–6°S, 160°–165°E, and a relative SST minimum of 29.4°C developed near the equator between 145° and 150°E. Strongest cooling occurred below the axis of the wind burst in the region between about 2°N and 2°S, 145°–160°E, with a maximum SST drop of over 0.5°C (Figure 14c). This pattern of cooling reinforces our conclusion based on the mooring time series (section 4.1), that variations in local air-sea heat flux were significant in determining the observed SST variability near the equator. Lateral advection was likely to be of secondary importance, since nowhere in the region (except at 8°N, 165°E) was water colder than 29.4°C found prior to the onset of strong westerly winds in mid-November. We note furthermore that this surface cooling occurred at a time of equatorial downwelling favorable westerly winds. If SST were strongly influenced by entrainment of cold water from the thermocline, we would have expected surface warming in late November since the thermocline was being displaced downward. The relative inefficiency entrainment from the thermocline in changing SST during westerly wind burst forcing is consistent with the existence of a salt stratified barrier layer as discussed in section 4.3.

5. SUMMARY AND DISCUSSION

Several 5 to 10 m s^{-1} westerly wind bursts of 10–15 days' duration occurred in the western equatorial Pacific between November 1989 and January 1990. The response to these wind bursts was characterized by a 400- to 600-km-wide eastward jet in the upper 100–150 m along the equator between 135°E and the date line. Flow in this jet accelerated to speeds of over 100 cm s^{-1} within 1 week after the onset of westerly winds in November 1989 in association with super-typhoon Irma. Separating this eastward flow near the surface from the Equatorial Undercurrent in the thermocline was a 20 to 40 cm s^{-1} westward counterflow which developed between 2°N and 2°S in response to wind burst forcing. These westerly wind-driven current variations resulted in a net zonal volume transport of 51 Sv to the east between 1.5°S and 5°N in the upper 150 m, compared with 5 Sv to the west prior to the onset of westerlies. A second wind burst in December 1989 resulted in volume transports over the same range of depths and latitudes of 20 Sv. Thus changes in surface layer zonal volume transports in the western Pacific due to westerly wind bursts in November and December 1989 were 25–56 Sv based on the three shipboard velocity sections we examined.

Westerly wind bursts produced convergent meridional velocities in the surface layer near the equator. In late November 1989, for example, $O(10$ cm s$^{-1})$ equatorward meridional velocities were observed along 165°E in both hemispheres within 3° of the equator, leading to a convergence of 1 × 10^{-6} s^{-1}. Zonal convergence in the eastward equatorial jet across 165°E was comparable in magnitude at this time, leading to a net horizontal convergence and downwelling at 15-m depth of 2–3 m d^{-1}. Associated with this convergence and downwelling, the thermocline was depressed by 20–30 m and sea level rose by 10 dyn cm.

Sea surface temperature cooling of 0.2°–0.5°C occurred over a large region of the western Pacific west of 170°E in response to wind burst forcing. The spatial pattern of this

cooling under the region of high wind speeds suggested an important role for evaporative heat flux during westerly bursts. It is also possible that reduced insolation contributed to the observed cooling, since westerly wind bursts are associated with enhanced convection and cloudiness. Consistent with these inferences, SST was observed to warm by about 0.5°C under light wind conditions (<2 m s^{-1}) between some episodes of westerlies. Lateral advection was probably of secondary importance despite the existence strong westerly wind-driven currents in the region, since horizontal SST gradients were generally weak in the warm pool; and water of 29.4°C (the minimum observed at the height of westerly wind forcing in late November 1989) was not found in reasonable proximity to the equator prior to the onset of westerlies. Entrainment from the thermocline was probably also of secondary importance in the surface layer heat balance on wind burst time scales owing to the existence of salt-stratified vertical buoyancy gradients in the upper 100 m. These gradients presumably diminished the effectiveness of vertical turbulent heat exchange with the thermocline and limited the depth penetration of surface heat fluxes. Thus temperatures in the upper 10 m responded rapidly to changing wind conditions, generally warming during light winds and cooling during high winds. Moreover, during episodes of peak wind speeds >8 m s^{-1} in December 1989 and January 1990, shallow haloclines supported the development of 0.2°–0.3°C sea surface temperature inversions. This indicates that a complete understanding the surface layer heat balance in the western Pacific will require information on salinity variations in order to determine the vertical scale over which heat exchange with the atmosphere takes place.

The most striking change in the salinity field along 165°E from November 1989 to January 1990 was a drop of over 1 psu in the surface layer near the equator immediately after the onset of westerlies. This change occurred over a span of about 10 days and was due primarily to equatorward advection of fresh water from north of the salinity front centered near 3°N. Other processes probably contributed to the observed equatorial surface layer salinity changes, although these processes were likely to be of secondary importance relative to meridional advection in late November 1989. For example, the rapidity with which the surface layer salinity decreased at the equator rules out enhanced freshwater flux at the air-sea interface as a primary causative mechanism. Specifically, the upper 101 m freshened by 1.0–0.6 psu during the 10 days following the onset of westerlies (Figure 6a). To account for this salinity change, net precipitation minus evaporation would have had to exceed the equivalent of 2 m of rainfall, or the annual average rainfall total near 0°, 165°E [Taylor, 1973]. Although it is likely that precipitation would be enhanced during westerly wind bursts in association with zonally convergent winds, low surface pressures, and high cloudiness [e.g., Lander and Morrissey, 1988], surface layer freshening due to precipitation would be partially offset by enhanced evaporation associated with high wind speeds. Hence it is improbable that there was 2 m of net freshwater flux across the air-sea interface in late November 1989 at 0°, 165°E. Similarly, vertical mixing may have created the 50-m-deep isohaline surface layer in Figure 10 but would not account for the net decrease in salinity registered over the upper 150 m between November and December 1989. Zonal advection due to the strong eastward jets evident in mooring, shipboard, and drifter data may have

produced some surface layer freshening along 165°E, although we have no suitably resolved zonal sections of salinity near the equator to determine gradients across 165°E for the study period. However, the observed surface salinity drop in late November, divided by a jet speed of 100 cm s^{-1}, would imply about a 1-psu salinity decrease in 10° of longitude to the west of 165°E. The sign of the inferred zonal gradient is consistent with the climatological surface salinity field in the western equatorial Pacific, but the magnitude is 5 times larger than expected [Levitus, 1986].

Linear equatorial theory predicts that the dynamical response to westerly wind burst forcing should initially involve a meridionally convergent, eastward accelerating Yoshida jet in the surface layer [Moore and Philander, 1977]. This jet would reach very high speeds in a short period of time because Coriolis forces are ineffective at retarding and deflecting currents near the equator. Superimposed on this jet would be a spectrum of inertia-gravity waves and, if the winds were not strictly zonal or if they were asymmetric about the equator, mixed Rossby-gravity waves. At later times in the evolution of the current field, equatorial Kelvin and long Rossby waves excited at the zonal extremes of the wind burst would propagate into the directly forced region and lead to decelerations of the eastward jet. The flow field should also be characterized by strong vertical shear across the surface layer due to downward turbulent diffusion of zonal momentum from the surface winds [McCreary, 1985].

Aspects of these dynamics have been identified in earlier descriptions of the response to wind burst forcing [e.g., McPhaden et al., 1988, 1990a] and similar dynamics were probably operative between November 1989 and January 1990. For instance, the strength of the eastward surface jet should be governed at least initially by the strength of the local zonal winds, and qualitatively we find this to be true in the present study. The weakest of the eastward surface jets occurred in January 1990 in association with relatively weak and sporadic local westerlies, whereas the strongest surface jet occurred in November 1989 during sustained and relatively strong local westerlies (Figure 4). Indirect evidence for nonlocally forced Kelvin and Rossby wave responses may also be found in the differences in amplitude and timing of the surface layer current variations in relation to the local winds. Local maximum westerly wind speeds were comparable during the November and December wind bursts, for instance, although westerlies were stronger and appeared earlier to west and north of 0°, 165°E, during the November wind event (Figure 3). These differences in the regional wind field would have lead to differences in the relative magnitude of remotely forced responses along 165°E and may be part of the reason why the maximum eastward speeds and transports of the surface jet were about twice as large in November as in December 1989. Hemispheric asymmetry in the zonal wind field may also have excited large-scale inertia-gravity waves and mixed Rossby-gravity waves which caused the surface zonal jet to meander around the equator as suggested by Figures 8 and 13.

The Equatorial Undercurrent decelerated to less than 20 cm s^{-1} (i.e., less than half its speed before the onset of westerlies) by early December 1989. Compared to current variations in the surface layer though, changes in EUC speed were generally smaller and not as clearly related to local wind forcing. For example, the EUC slowly accelerated from mid-December 1989 to the end of January 1990, despite

the occurrence of frequent westerly winds. The relative insensitivity of zonal flow in the thermocline to local surface wind forcing at 0°, 165°E, was noted previously by *McPhaden et al.* [1990a] in the context of variability during the 1986–1987 ENSO. These results suggest that changes in EUC speed due to wind burst forcing are probably more related to remotely forced equatorial wave processes which alter the zonal pressure gradient in the thermocline.

Previous analysis has indicated that wind burst forcing may be associated with enhanced vertical turbulent viscosity of $O(100 \text{ cm}^2 \text{ s}^{-1})$ in the surface layer [*McPhaden et al.*, 1988]. Consistent with this result, we found that strong vertical shears developed down to 150 m in response to westerly wind events between November 1989 and January 1990. Thus it appears that shallow haloclines in the warm pool may be less effective in limiting the vertical penetration of momentum than the vertical penetration of heat. If so, this suggests a possible role for small-scale internal waves in mediating vertical turbulent momentum transports as recently described in the context of mixing studies in the eastern equatorial Pacific [*Wijesekera and Dillon*, 1991; *Moum et al.*, 1992; *McPhaden and Peters*, 1992].

The period of our study coincided with a rapidly falling Southern Oscillation Index (SOI) which reached its lowest value in 10 years (excluding the 1982–1983 ENSO) in February 1990 [*Climate Analysis Center*, 1991]. In addition, although there was localized cooling in response to wind burst forcing west of 170°E, 0.5°–1.0°C warm SST anomalies developed in early 1990 near the date line, where we observed strong zonal convergence of the eastward jets. Westerly bursts also excited equatorial Kelvin waves which could be traced using mooring data into the eastern Pacific [*Weisberg et al.*, 1990]. However, deep atmospheric convection did not subsequently develop over the anomalously warm SSTs near the date line, nor did warm SST anomalies develop in the equatorial cold tongue of the eastern Pacific. Moreover the SOI, which had been low primarily because of high surface pressure at Darwin, Australia, rebounded toward zero after February 1990. Thus in spite of evolving ENSO-like conditions in the western Pacific associated with wind burst forcing in late 1989 to early 1990, an ENSO failed to occur.

Recent experiments with coupled ocean-atmosphere models suggest that short-time-scale wind variations in the western Pacific may not be an essential component of the ENSO cycle [*Zebiak*, 1989]. These same coupled ocean-atmosphere models (which do not explicitly simulate synoptic-scale atmospheric wind fluctuations) predicted near-normal SSTs in the eastern and central equatorial Pacific for 1990, in agreement with the observations [*Kerr*, 1991]. Thus the critical role of westerly wind bursts in the ENSO cycle is debatable. However, regardless of the detailed influence (if any) of wind bursts on climate variability, there is no doubt about their dramatic effect on upper ocean current, temperature, and salinity structures in the western equatorial Pacific.

APPENDIX: INSTRUMENTATION AND DATA PROCESSING

A1. Current Meter Mooring Data at 0°, 165°E

Currents and temperatures were measured from a taut-line surface mooring with six model 610 EG&G vector averaging

current meters (VACMs) evenly spaced between 50 and 300 m, and an EG&G vector measuring current meter (VMCM) at 10-m depth. Subsurface temperatures were measured at seven additional depths in the upper 500 m with SeaData temperature recorders. Temperature at 1 m below the surface, nominally referred to as SST, was also measured. Winds were determined from an R. M. Young model 05103 propeller and vane mounted at 4-m height on the surface toroid. Data were internally recorded at intervals of 15 min to 2 hours depending on instrument type. In addition, surface winds, SST and 10-m currents were telemetered to shore via Service Argos. Instrumental accuracies are a few centimeters per second for current speeds, 0.01°–0.05°C for temperatures, and 0.1–0.2 m s^{-1} for wind speeds. Further details of data processing and instrumental accuracies for winds, currents, and temperature are given by *McPhaden et al.* [1990a] and *Feng et al.* [1991].

The current meter data spanned two mooring deployments: CU-7 from May 20 until November 15, 1989, and CU-8 from November 17, 1989, until June 20, 1990. Mooring CU-7 was instrumented with three SeaBird SBE-16 SEACAT conductivity and temperature recorders, one each at 11 m, 51 m, and 101 m. This vertical array was augmented with three additional SEACATs on mooring CU-8 at depths of 3 m, 30 m, and 75 m. Conductivity and temperature were sampled every 30 min and converted to salinity using standard algorithms after recovery. Predeployment and postdeployment laboratory calibrations and in situ comparisons with CTD data suggest that the instruments were accurate to within the manufacture's specifications of a 0.01°C and 0.006 S m^{-1} (approximately 0.06 psu in salinity) over 6 months. Additional information on the performance of moored SEACATs in the equatorial Pacific is given by *McPhaden et al.* [1990b].

A2. ATLAS Thermistor Chain Mooring Data

The ATLAS mooring is a taut-line surface mooring similar in design to the 165°E current meter mooring. The ATLAS measured surface winds at 4-m height with an R. M. Young propeller and vane assembly, SST at 1-m depth, 10 subsurface temperatures in the upper 500 m, and 2 subsurface pressures. All data were internally recorded and telemetered to shore via Service Argos. Winds were averaged over 6-hour intervals, and temperatures were averaged over 24-hour intervals. Instrumental accuracies for temperature and winds are similar to those for the current meter mooring. Further details on ATLAS mooring design and data processing are given by *Hayes et al.* [1991].

A3. Circulation Drifter Data

Up to 30 circulation drifters drogued at 15-m depth populated the study region from November 1989 to January 1990. Some of these drifters were launched prior to November 1989 as part of the ongoing Pan-Pacific drifters experiment [*Niiler*, 1990]. In addition, 12 circulation drifters were launched on U.S.-PRC 7 between 141°E and 165°E in November 1989, and 13 circulation drifters were launched on SURTROPAC 13 in December 1989. Each buoy measured SST from a thermistor located in the buoy hull. Buoy positions were determined via Service Argos, and both position and SST data were transmitted to shore every 3

days. Velocities were calculated from these position data interpolated to 6-hourly values. The drifters follow the currents at drogue depth to within about 2 cm s^{-1} (P. P. Niiler et al., Measurements of the water following capability of holey-sock and tristar drifters, submitted to *Journal of Atmospheric and Oceanic Technology*, 1991); thermistors calibrated prior to deployment indicate an accuracy of 0.1°C for SST.

A4. Drifting Thermistor Chain Data

In October–November 1989, 21 drifting buoys with 300-m-long thermistor chains were deployed from the *Xiangyanghong #14* as indicated in Figure 1. Of these drifters, 19 were manufactured by Polar Research Laboratory (PRL) of Carpenteria, California, and 2 were manufactured by TECHNOCEAN of San Diego, California. Each drifter was equipped with an SST sensor on the buoy hull, 12 subsurface temperature sensors, and 3 subsurface pressure sensors. Temperature and pressure data were telemetered to satellite via Service Argos as 3-hour averages. Position fixes were available about 6 times per day, with a standard error of 350 m 72% of the time.

In this study we use only position data, which were time differenced to infer drifter velocities, and SST data, which were accurate to about 0.04°C based on predeployment laboratory calibrations. Drift velocities result from a vertical integral of the drag forces over the buoy hull and 300-m-long thermistor chain. Hence these drifters do not follow the near-surface flow field as closely as the circulation drifters discussed above. However, in response to wind burst forcing the largest changes in circulation occur in the upper 100 m, which will dominate drag forces on the thermistor chain. We expect therefore that the drifting thermistor chain velocities will provide a qualitative indicator of both magnitude and direction of the near-surface flow. Further discussion of the PRL buoy systems and data processing procedures is given by *McPhaden et al.* [1991].

A5. Acoustic Doppler Current Profiler (ADCP) Data

Velocity profile data were collected continuously on U.S.-PRC 7, leg 2 (Ponape to Guam), in November 1989 with a 153.6-kHz RD Instruments ADCP. The instrument provided high-quality data over of depth range of typically 20–400 m with approximately 16-m vertical resolution. Absolute velocities in Earth coordinates were obtained by combining the ADCP relative velocities with heading information from the ship's gyrocompass and navigation data from TRANSIT satellite fixes. Data were then averaged to 0.5° latitudinal intervals for subsequent analysis. A comparison of the shipboard ADCP and moored velocity measurements at 0°, 165°E in November 1989 indicates typical rms differences of 6 cm s^{-1}. Further information on data collection, editing and processing, is given by *Bahr et al.* [1992].

A6. Aanderaa Profiling Current Meter Data

Velocity data along 165°E on SURTROPAC 13 were obtained with an Aanderaa RCM-7 profiling current meter that freely slid down a 600-m cable under a drifting buoy. The RCM-7 profiler system was ballasted to remain vertical while sinking at roughly 7–10 m min^{-1}. At the bottom of the cable, another RCM-7 current meter was mounted to deter-

mine the drift of the buoy system relative to flow at 600 m (which was assumed to be negligible). Horizontal current velocities as a function of depth were then inferred from velocity differences between the profiling RCM-7 and the 600-m RCM-7. Stations were occupied approximately every 0.5° of latitude between 5°N and 5°S and every 1° of latitude poleward of 5°. Vertical resolution of the velocity profiles is 5 m.

The errors inherent in this kind of measurement are roughly 10–20 cm s^{-1}. *McPhaden and Picaut* [1990], for example, found typical root-mean-square (rms) zonal velocity differences of 15–20 cm s^{-1} between moored measurements and 7 Aanderaa profiles within 3 km of the 165°E current meter mooring in June 1986 and July 1988. *Delcroix et al.* [1992] found rms differences of 13 cm s^{-1} (9 cm s^{-1}) for zonal (meridional) velocities based on 15 contemporaneous Aanderaa and ADCP profiles within 2–3 km of one another between 7°N and 10°S in March 1991. In both cases, a significant percentage of the rms difference was due to vertical mean differences between the measurements. When referenced to the same depths, for example, the differences between Aanderaa and ADCP profiles reported by Delcroix et al. reduced to 8 cm s^{-1} (6 cm s^{-1}) in the zonal (meridional) direction. Further discussion of the instrument and sampling characteristics is given by *du Penhoat et al.* [1990].

A7. Conductivity-Temperature-Depth (CTD) Data

Hydrographic observations on U.S.-PRC 7 were obtained with an EG&G Marine Systems Mark III conductivity-temperature-depth instrument (CTD) equipped with a polarographic dissolved oxygen sensor. Station work along longitude 165°E began at 10°N on November 12, reaching the equator on November 15 and 7°S on November 19. Thereafter, the cruise track turned southwest; the final station on the leg at 10°30'S 162°10'E was completed on November 21. Stations were taken to a nominal depth of 3000 m (or to within 100–200 m of the ocean bottom where shallower). Station spacing was 0.5° of latitude equatorward of 3°, and about 1° of latitude poleward of 3°. Temperature and pressure sensor calibration information for these data were derived from laboratory measurements at the calibration facilities of EG&G and the Woods Hole Oceanographic Institution. Salinity and oxygen data were calibrated relative to water samples obtained from a rosette sampler and analyzed at sea, with reference to the historical deep water property distributions. A calibrated data set with 2-dbar vertical resolution was produced for subsequent analysis. The pressure, temperature, salinity, and oxygen uncertainty of these data are believed to be ±5 dbar, 0.003°C, 0.005 psu, and 0.1 mL L^{-1}, respectively. The techniques for reduction and calibration of the observations are discussed in the data report of *Lake et al.* [1991].

Hydrographic data were collected on SURTROPAC 13 using a wire-lowered SeaBird SBE-9 CTD. Station spacing was approximately every 0.5° of latitude between 5°S and 4°N, and every 1° poleward of these latitudes. Laboratory calibrations of temperature and conductivity sensors were performed in August 1989 and January 1989 respectively by SeaBird, Inc. In addition, salinity measurements were calibrated relative to water samples collected and analyzed at sea during SURTROPAC-13. Calibrated data were processed to 5-dbar vertical resolution for subsequent analysis.

Accuracy is expected to be comparable to that of the U.S.-PRC data in the upper 1000 m. Further details are given by *du Penhoat et al.* [1990].

A8. *Island Winds*

Wind data were collected from Nauru and Kapingamarangi islands with an R. M. Young model 05103 propeller and vane assembly mounted on a tower 10 m above the ground. These anemometers were replaced every 6–12 months and are calibrated prior to deployment to within 0.2 m s^{-1}. Data were vector averaged for 40 min each hour, then three individual hourly samples were transmitted to shore via GOES geostationary satellite.

The wind sensor at Kapingamarangi is located on the east side of the lagoon on a coral head that outcrops at low tide. We assume that air flow is relatively unobstructed at this location, although there are some small palm-covered islands within a few kilometers of the wind sensor. At Nauru, winds before February 1988 were measured only on the east side of the island in the lee (for westerly winds) of a 40-m hill. This led to wind speeds that were biased low during periods of westerlies [*McPhaden et al.*, 1988]. To alleviate this problem, a second wind sensor was installed in a relatively flat area on the west side of the island in February 1989. These winds are more representative of open ocean conditions during westerly events and are used exclusively in this study.

REFERENCES

Bahr, F., E. Firing, and S.-N. Songian, Acoustic Doppler current profiling in the western Pacific during the US-PRC TOGA cruises 7 and 8, technical report, Joint Inst. for Mar. and Atmos. Res., Univ. of Hawaii, Honolulu, in press, 1992.

Climate Analysis Center, Climate diagnostics bulletin, Near real-time analyses, January 1991, 63 pp., Natl. Oceanic and Atmos. Admin., U. S. Dep. of Commer., Washington, D. C., 1991.

Delcroix, T., and C. Henin, Observations of the Equatorial Intermediate Current in the western Pacific Ocean, *J. Phys. Oceanogr.*, *18*, 363–366, 1988.

Delcroix, T., and C. Hénin, Seasonal and interannual variations of sea surface salinity in the tropical Pacific Ocean, *J. Geophys. Res.*, *96*, 22,135–22,150, 1991.

Delcroix, T., G. Eldin, and C. Hénin, Upper ocean water masses and transports in the western tropical Pacific (165°E), *J. Phys. Oceanogr.*, *17*, 2248–2262, 1987.

Delcroix, T., F. Masia, and G. Eldin, Comparison of profiling current meter and shipboard ADCP measurements in the western equatorial Pacific, *J. Atmos. Ocean. Technol.*, in press, 1992.

Delcroix, T., G. Eldin, M.-H. Radenac, J. Toole, and E. Firing, Variation of the western equatorial Pacific Ocean, 1986–1988, *J. Geophys. Res.*, *97*, 5423–5446, 1992.

Donguy, J.-R., and A. Dessier, El Niño-like events in the tropical Pacific, *Mon. Weather Rev.*, *111*, 2136–2139, 1983.

du Penhoat, Y., F. Gallois, M.-J. Langlade, G. Reverdin, and H. Walico, Rapport de la campagne SURTROPAC-13 à bord du N.O. *Le Suroit*, 167 pp., Inst. Fr. de Rech. Sci. pour le Develop. en Coop. (ORSTOM), Nouméa, New Caledonia, 1990.

Feng, Y., H. P. Freitag, M. J. McPhaden, and A. J. Shepherd, Wind, current and temperature data at 0°, 165°E: January 1986 to March 1991, *NOAA Data Rep. ERL PMEL-36*, 54 pp., Pac. Mar. Environ. Lab., Seattle, Wash., 1991.

Harrison, D. E., and B. S. Giese, Episodes of surface westerly winds as observed from islands in the western tropical Pacific, *J. Geophys. Res.*, *96*, suppl., 3221–3237, 1991.

Harrison, D. E., and P. S. Schopf, Kelvin wave induced anomalous advection and the onset of surface warming in El Niño events, *Mon. Weather Rev.*, *112*, 923–933, 1984.

Hayes, S. P., L. J. Mangum, J. Picaut, A. Sumi, and K. Takeuchi, TOGA-TAO: A moored array for real-time measurements in the tropical Pacific Ocean, *Bull. Am. Meteorol. Soc.*, *72*, 339–347, 1991.

Hisard, P., J. Merle, and B. Voituriez, The Equatorial Undercurrent at 170°E in March and April 1967, *J. Mar. Res.*, *28*, 281–303. 1970.

Keen, R. A., The role of cross-equatorial tropical cyclone pairs in the Southern Oscillation, *Mon. Weather Rev.*, *110*, 1405–1416, 1982.

Keen, R. A., Equatorial westerlies and the Southern Oscillation, in Proceedings of the U.S. TOGA Western Pacific Air-Sea Interaction Workshop, edited R. Lukas and P. Webster, *Tech. Rep. USTOGA-8*, pp. 121–140, Univ. Corp. for Atmos. Res., Boulder, Colo., 1988.

Kerr, R. A., El Niño winners and losers declared, *Science*, *251*, 1182, 1991.

Lake, B. J., K. Yang, Z. Luizhi, R. C. Millard, S. Pu, J. M. Toole, Z. Wang, and L. J. Mangum, Hydrographic observations from the US/PRC Cooperative Program in the western equatorial Pacific Ocean: Cruises 5–8, *Tech. Rep. WHOI-91-19*, Woods Hole Oceanogr. Inst., Woods Hole, Mass., 1991.

Lander, M. A., and M. L. Morrissey, Genesis of twin typhoons associated with a west wind burst in the equatorial western Pacific: A case study, in Proceedings of the U.S. TOGA Western Pacific Air-Sea Interaction Workshop, *Tech. Rep. USTOGA-8*, pp. 163–174, Univ. Corp. for Atmos. Res., Boulder, Colo., 1988.

Levitus, S., Annual cycle of salinity and salt storage in the world ocean, *J. Phys. Oceanogr.*, *16*, 322–343, 1986.

Lukas, R., and E. Lindstrom, The mixed layer of the western equatorial Pacific Ocean, *J. Geophys. Res.*, *96*, suppl., 3343–3357, 1991.

Luther, D. S., D. E. Harrison, and R. A. Knox, Zonal winds in the central equatorial Pacific and El Niño, *Science*, *222*, 327–330, 1983.

McCreary, J. P., Jr., Modeling equatorial ocean circulation, *Annu. Rev. Fluid Mech.*, *17*, 359–409, 1985.

McPhaden, M. J., and S. P. Hayes, Variability in the eastern equatorial Pacific during 1986–1988, *J. Geophys. Res.*, *95*, 13,195–13,208, 1990.

McPhaden, M. J., and S. P. Hayes, On the variability of winds, sea surface temperature and surface layer heat content in the western equatorial Pacific, *J. Geophys. Res.*, *96*, suppl., 3331–3342, 1991.

McPhaden, M. J., and H. Peters, On the diurnal cycle of internal wave variability in the eastern equatorial Pacific: Results from moored observations, *J. Phys. Oceanogr.*, in press, 1992.

McPhaden, M. J., and J. Picaut, El Niño/Southern Oscillation displacements of the western equatorial Pacific warm pool, *Science*, *250*, 1385–1388, 1990.

McPhaden, M. J., H. P. Freitag, S. P. Hayes, B. A. Taft, Z. Chen, and K. Wyrtki, The response of the equatorial Pacific to a westerly wind burst in May 1986, *J. Geophys. Res.*, *93*, 10,589–10,603, 1988.

McPhaden, M. J., S. P. Hayes, L. J. Mangum, and J. M. Toole, Variability in the western equatorial Pacific Ocean during the 1986–87 El Niño/Southern Oscillation event., *J. Phys. Oceanogr.*, *20*, 190–208, 1990a.

McPhaden, M. J., H. P. Freitag, and A. J. Shepherd, Moored salinity time series measurements at 0°, 140°W, *J. Atmos. Ocean. Technol.*, *7*, 568–575, 1990b.

McPhaden, M. J., A. J. Shepherd, W. G. Large, and P. P. Niiler, A TOGA array of drifting thermistor chains in the western equatorial Pacific Ocean: October 1989–January 1990, *NOAA Data Rep.*

ERL PMEL-34, 171 pp., Pac. Mar. Environ. Lab., Seattle, Wash., 1991.

Miller, L., R. Cheney, and B. Douglas, Geosat altimeter observations of Kelvin waves and the 1986–87 El Niño, *Science, 239*, 52–54, 1988.

Moore, D. W., and S. G. H. Philander, Modeling of the tropical ocean circulation, in *The Sea*, vol. 6, *Marine Modelling*, edited by E. D. Goldberg et al., pp. 319–361, Wiley-Interscience, 1977.

Moum, J. N., D. Hebert, C. A. Paulson, and D. R. Caldwell, Turbulence and internal waves at the equator, 1, Statistics from towed thermistors and a microstructure profiler, *J. Phys. Oceanogr.*, in press, 1992.

Niiler, P. P., Drifter observations, mass, heat and vorticity divergence in the tropical Pacific, 1988–1989, in International TOGA Scientific Conference Proceedings, *Rep. WCRP-43*, p. 71, World Meteorol. Organ., Geneva, 1990.

Nitta, T., and T. Motoki, Abrupt enhancement of convective activity and low-level westerly burst during the onset phase of the 1986–87 El Niño, *J. Meteorol. Soc. Jpn.*, *65*, 497–506, 1987.

Picaut, J., S. P. Hayes, and M. J. McPhaden, Use of the geostrophic approximation to estimate time-varying zonal currents at the equator, *J. Geophys. Res.*, *94*, 3228–3236, 1989.

Picaut, J., A. J. Busalacchi, M. J. McPhaden, and B. Camusat, Validation of the geostrophic method for estimating zonal currents at the equator from Geosat altimeter data, *J. Geophys. Res.*, *95*, 3015–3024, 1990.

Sui, C.-H., and K.-M. Lau, Multi-scale phenomena in the tropical atmosphere over the western Pacific, *Mon. Weather Rev.*, *120*, 407–430, 1992.

Taylor, R., An atlas of Pacific rainfall, *Tech. Rep. HIG-73-9*, 7 pp., Hawaii Inst. of Geophys., Univ. of Hawaii, Honolulu, 1973.

Weisberg, R. H., S. P. Hayes, and M. J. McPhaden, The evolution along the equator of wintertime zonal momentum pulses, *Eos Trans. AGU*, *71*, 1231, 1990.

Wijesekera, H., and T. M. Dillon, Internal waves and mixing in the upper equatorial Pacific Ocean, *J. Geophys. Res.*, *96*, 7115–7126, 1991.

Wyrtki, K., and G. Meyers, The tradewind field over the Pacific Ocean, 1, The mean field and annual mean variation, *Tech. Rep. HIG-75-1*, 26 pp., Hawaii Inst. of Geophy., Univ. of Hawaii, Honolulu, 1975.

Zebiak, S., On the 30–60-day oscillation and the prediction of El Niño, *J. Clim.*, *2*, 1381–1387, 1989.

F. Bahr, P. L. Richardson, and J. M. Tode, Woods Hole Oceanographic Institution, Woods Hole, MA 02543.

Y. du Penhoat, Groupe SURTROPAC, ORSTOM, B.P. A5, Nouméa, New Caledonia.

E. Firing, Hawaii Institute of Geophysics, University of Hawaii, 1000 Pope Road, Honolulu, HI 96822.

S. P. Hayes and M. J. McPhaden, Pacific Marine Environmental Laboratory, NOAA, Building 3, 7600 Sand Point Way NE, Seattle, WA 98115.

P. P. Niiler, Scripps Institution of Oceanography, La Jolla, CA 92093.